Three Dimensional Quantum Dynamics of (H^-, H_2) and Its Isotopic Variants

Aditya Narayan Panda, Kousik Giri, and N. Sathyamurthy*

Department of Chemistry, Indian Institute of Technology Kanpur, Kanpur 208016, India

Received: November 4, 2004; In Final Form: January 6, 2005

We present the results of a time-dependent quantum mechanical investigation using centrifugal sudden approximation in the form of reaction probability as a function of collision energy (E_{trans}) in the range 0.3−3.0 eV for a range of total angular momentum (J) values and the excitation function $\sigma(E_{trans})$ for the exchange reaction $H^- + H_2$ ($v = 0, j = 0$) → $H_2 + H^-$ and its isotopic variants in three dimensions on an accurate ab initio potential energy surface published recently (*J. Chem. Phys.* **2004**, *121*, 9343). The excitation function results are shown to be in excellent agreement with those obtained from crossed beam measurements by Zimmer and Linder for $H^- + D_2$ collisions for energies below the threshold for electron detachment channel and somewhat larger than the most recent results of Haufler et al. for (H^-, D_2) and (D^-, H_2) collisions.

I. Introduction

Collisions of positive, neutral and negatively charged hydrogen atoms with hydrogen molecules constitute an important subject of study from a fundamental point of view. They represent ideal prototype systems for a detailed comparison between theory and experiment. They are also of interest in understanding the collision processes in interstellar media and in plasmas. H_3^+ [1−3] is known to be stable. The ground-state potential-energy surface (PES) has a well of depth 4.61 eV, which supports a large number of bound states that affect the dynamics of the system. The PES for the neutral counterpart H_3, on the other hand, has a barrier of 0.45 eV for the exchange reaction.[4] The dynamics of (H, H_2) collisions have been studied extensively over the years.[5,6] In comparison, the (H^-, H_2) system has been studied much less. Qualitatively, the PES of H_3^- is very similar to that of H_3 in many ways, including the barrier height. However, there are also differences between the two systems. At large center-of-mass separation between H^- and H_2, the charge-induced dipole interaction between the two leads to a shallow well of depth around 0.05 eV. The additional electron in H_3^- gives rise to an additional reaction channel involving electron detachment. Although the electron affinity of H atom is 0.75 eV,[7] no detachment occurs at this energy as there is no crossing between the ground-state PESs for H_3 and H_3^- at large distances. For H_2 in its ground electronic state, the crossing between the two PESs occur at short distances.[8] As a result, electron detachment is expected[9] to occur around 1.45 eV, through the following pathway:

$$H^- + H_2 \rightarrow [H_3^-]^{\neq} \rightarrow H + H_2 + e^-$$

Muschlitz et al.[10] and Mason and Vanderslice[11] measured elastic and inelastic integral cross sections for (H^-, H_2) collisions and attributed their results to the strong long-range ion−molecule polarization effects. Michels and Paulson[12] measured the reaction cross section (σ) for $H^- + D_2$ (HD) and $D^- + H_2$ (HD) collisions using the tandem mass spectrometer (TMS). A reaction threshold of approximately 1.0 eV was found, and a plot of the excitation function exhibited a maximum around 3.0 eV. Huq et al.[13] measured total reaction cross sections for the reactive and the electron detachment channels for collisions of H^- and D^- with H_2, D_2 and HD. The electron detachment threshold was found to be 1.45 eV for (H^-, H_2). Zimmer and Linder[14] determined the integral reaction cross section for (H^-, D_2) collisions by crossed beam studies and concluded that the decrease in reaction cross section when plotted as a function of collision energy (E_{trans}) at higher energies arose because of the opening up of the electron detachment channel. They attributed the differences between their results and that of Michels and Paulson to the deficiency in the TMS measurements. They also measured the elastic and rotationally inelastic (nonreactive) and electron detachment cross sections. Müller et al.[15] performed crossed-beam measurements of rotationally inelastic scattering of H_2 from H^- and obtained state-specific differential cross sections for transitions ranging from initial rotational state j_i = 1−3 to final state j_f = 1−13, for the ground vibrational (v = 0) state of H_2. Their results showed a strong rotational excitation of the target molecule. Haufler et al.[16] determined the integral cross sections for $H^- + D_2$ and $D^- + H_2$ reactions using a guided beam apparatus and noted a significant isotope effect.

There have been a number of theoretical studies on the electronic structure of H_3^-. Particularly worth mentioning is the diatomics-in-molecules (DIM) potential energy surface computed by Belyaev et al.[17] and a multireference-configuration-interaction study by Stärck and Meyer.[9] While Belyaev et al.[17] computed state-to-state reaction probabilities for the collinear configuration of (H^-, H_2) and (H^-, D_2) using the DIM surface, Mahapatra et al.[18] found that there were a large number of transition state resonances on the Stärck-Meyer (SM) PES for $H^- + H_2$ in collinear geometry. Presence of a large number of resonances in the system was confirmed by time-dependent quantum mechanical (TDQM)[19,20] calculations for collinear as well as three-dimensional arrangements.[21] Quasiclassical trajectory calculations carried out by Ansari and Sathyamurthy[22] for the collinear geometry yielded results in good agreement with the TDQM results. Gianturco and Kumar[23] calculated the differential and integral cross sections for vibrationally inelastic processes in ($H^- + H_2$) collisions over a wide range of collision energy (4.67−40 eV) on the SM PES. Mahapatra[24] carried out three-dimensional TDQM calculations on the DIM PES and

* Corresponding author. E-mail: nsath@iitk.ac.in.

10.1021/jp044953l CCC: $30.25
Published on Web 02/16/2005

found the existence of sharp resonances near the threshold for rovibrationally excited reactant molecules, particularly for $v = 2$, $j = 0-3$. Jaquet and Heinen[25] performed full three-dimensional TDQM calculations for total angular momentum $J = 0$ on both the DIM and SM surfaces and showed that the narrow resonances in the reaction probability plot were smeared, when averaged over J, using the J-shifting approximation.

We have carried out a TDQM investigation of three-dimensional collisions of (H^-, H_2 ($v = 0$, $j = 0$)) and its isotopic variants for a range of J values on a recently reported ab initio PES by Panda and Sathyamurthy,[26] for collision energy in the range 0.3−3.0 eV, and compared the results with the experimental results, wherever available. We outline the theoretical methodology briefly in section II, and the results obtained are presented and discussed in section III. A summary of our findings and the conclusion follow in section IV.

II. Methodology

Different aspects of the TDQM wave packet (WP) methodology are well documented in the literature.[19,20] Therefore, we present only the salient features of our calculation here. We have used an L-shaped grid[27,28] in reactant channel Jacobi coordinates (R, r, γ), where R is the center-of-mass separation between H^- and H_2, r is the bond distance in H_2, and γ is the angle between R and r. The Hamiltonian in (R, r, γ) for a given J and $j = 0$ in the body-fixed frame is given by

$$\hat{H} = -\frac{\hbar^2\partial^2}{2\mu_R\partial R^2} - \frac{\hbar^2\partial^2}{2\mu_r\partial r^2} + \frac{\mathbf{J}^2}{2\mu_R R^2} + V(R,r,\gamma) \qquad (1)$$

Here μ_R is the reduced mass of H^- with respect to H_2 and μ_r the reduced mass of H_2. $\mathbf{J}$ is the total angular momentum operator and $V(R, r, \gamma)$ is the three-body interaction potential reported by Panda and Sathyamurthy.[26]

The initial WP, $\Psi(R,r,\gamma,t=0)$, is chosen as the product of a Gaussian wave packet ($G_{k_0}(R)$), representing the translational motion of H^- with respect to H_2, a ground ro-vibrational ($v = 0$, $j = 0$) eigenfunction $\phi_{vj}(r)$ for the diatom and a normalized associated Legendre polynomial $\tilde{P}_{jK}(\cos\gamma)$:

$$\Psi(R,r,\gamma,t=0) = G_{k_0}(R)\phi_{vj}(r)\tilde{P}_{jK}(\cos\gamma) \qquad (2)$$

The translational wave packet is a Gaussian function of the form

$$G_{k_0}(R) = \left(\frac{1}{\pi\delta^2}\right)^{1/4} \exp(-(R-R_0)^2/2\delta^2)\exp(-ik_0R) \qquad (3)$$

where R_0 and δ refer to the location of the center of the WP and the width parameter, respectively. The momentum wave vector k_0 is related to the initial translational energy through the relation[32]

$$k_0 = \sqrt{\frac{2\mu_R E_{trans}}{\hbar^2} - \frac{1}{2\delta^2}} \qquad (4)$$

The values of δ and k_0 are chosen in accordance with the initial energy distribution desired.

The radial part of the diatomic ro-vibrational eigenfunction $\phi_{vj}(r)$ is computed by means of the Fourier grid Hamiltonian approach proposed by Marston and Balint-Kurti.[33]

The normalized associated Legendre polynomials

$$\tilde{P}_{jK}(\cos\gamma) = \sqrt{\frac{(2j+1)(j-K)!}{2(j+K)!}}P_{jK}(\cos\gamma) \qquad (5)$$

are eigenfunctions of the $\mathbf{j}^2$ operator with eigenvalues $j(j+1)\hbar^2$.

The fast Fourier transform algorithm[29] is used to evaluate the effect of the radial part of the kinetic energy operator on the wave function and the discrete variable representation (DVR)[30] is used for the angular part. The split-operator method[32] is used for the propagation of the wave packet in time.

The action of the angular momentum operators (nondiagonal in the radial grid representation) on the WP is carried out in associated Legendre polynomial basis set $\tilde{P}_{jK}$. First, the WP is transformed through a DVR transformation, $T^K_{nj} = \sqrt{w_n}\tilde{P}_{jK}(\cos\gamma_n)$. Then the matrix elements are evaluated as

$$\langle\tilde{P}_{jK}|\mathrm{j}^2|\tilde{P}_{j'K'}\rangle = \delta_{jj'}\delta_{K,K'}\hbar^2 j(j+1) \qquad (6)$$

$$\langle\tilde{P}_{jK}|\mathbf{J}^2|\tilde{P}_{j'K'}\rangle = \hbar^2\delta_{jj'}\{[J(J+1)+j(j+1)-2K^2]\delta_{K,K'} - \lambda_{JK}{}^{+}\lambda_{jK}{}^{+}\sqrt{1+\delta_{K0}}\delta_{K+1,K'} - \lambda^-_{JK}\lambda^-_{jK}\sqrt{1+\delta_{K1}}\delta_{K-1,K'}\} \qquad (7)$$

where the quantity λ is defined as

$$\lambda^{\pm}_{AB} = \sqrt{A(A+1) - B(B\pm 1)} \qquad (8)$$

Here K is the projection of J on the body-fixed z axis and for a given J and j, K varies in the range $0 \le K \le \min(J, j)$. It is worth pointing out here that the projection of j on the body-fixed z-axis is equal to K, as l_z, the projection of l on the body-fixed z-axis is zero, in the chosen body-fixed axis. The final expression is obtained by transforming back to the DVR.

Within the centrifugal sudden approximation,[31] the off-diagonal terms in K are neglected. The angular kinetic energy operator then reads as

$$\hat{T}(\gamma) = \frac{\hbar^2}{2\mu_R R^2}[J(J+1)+j(j+1)-2K^2] + \frac{\hbar^2}{2\mu_r r^2}j(j+1) \qquad (9)$$

Having computed the wave function $\Psi(t)$ at time t, the energy resolved reaction probability ($P(E)$) is calculated from the total flux through a surface located in the product channel at $r = r_s$ as follows:[34]

$$P(E) = \frac{\hbar}{\mu_r}\mathrm{Im}\left[\int_0^\infty \mathrm{d}R\int_0^\pi \mathrm{d}\theta\,\sin\theta\Psi^*(R,r,\theta,E)\frac{\mathrm{d}}{\mathrm{d}r}\Psi(R,r,\theta,E)\right]_{r=r_s} \qquad (10)$$

The energy dependence of the wave function in eq 10 is obtained by Fourier transforming the time-dependent wave packet as

$$\Psi(R,r,\theta,E) = \frac{1}{a_E}\int_{-\infty}^{\infty}\exp(iEt/\hbar)\Psi(R,r,\theta,t)\,\mathrm{d}t \qquad (11)$$

with a_E as the normalization factor. The latter corresponds to the weight of the energy component contained in the initial translational WP and is defined by

$$a_E = \left(\frac{\mu_R}{\hbar k}\right)^{1/2}\int_{-\infty}^{\infty} G_{k_0}(R)\exp(ikR)\,\mathrm{d}R = \left(\frac{\mu_R}{\hbar k}\right)^{1/2} G_{k_0}(k) \qquad (12)$$

Here

$$G_{k_0}(k) = (4\pi\delta^2)^{1/4}\exp[-\delta^2(k-k_0)^2/2 + i(k-k_0)R_0] \qquad (13)$$

with $k_{vj} = \sqrt{2\mu_R(E-\epsilon_{v,j})}/\hbar$ and $\epsilon_{v,j}$ is the ro-vibrational energy of H_2.

TABLE 1: Parameters Used for the L-Shaped Grid and Initial Condition Details for $J \leq 8$ (See Text for $J > 8$)

parameters	values	
(N_{R1}, N_{R2})	(128, 64)	no. of grid points in R
$(R_{min}, R_{max})/a_0$	(1.0, 16.24)	range of R values
(N_{r1}, N_{r2})	(80, 48)	no. of grid points in r
$(r_{min}, r_{max})/a_0$	(0.4, 11.46)	range of r values
N_γ	54	no. of grid points in γ
$(R_{mask}, r_{mask})/a_0$	(14.08, 9.22)	starting point of the masking function along (R, r)
Δt/fs	0.2419	time step used in propagation
T/ps	0.97	total propagation time
R_0/a_0	(11.0)	centre of initial WP
E^0_{trans}/eV	1.0	initial translational energy
δ/a_0	0.25	Gaussian width parameter
r_s/a_0	6.0	position of the analysis surface in the product channel

The J-dependent reaction probability (P^J_{vj}) for the initial vib-rotational state (v, j) is computed from the initial (J, K) selected probability (P^{JK}_{vj}) as

$$P^J_{vj}(E) = \frac{1}{2j+1}[P^{JK=0}_{vj}(E) + 2\sum_{K=1}^{j} P^{JK}_{vj}(E)] \qquad (14)$$

However, the second term in eq 14 does not make any contribution in our present study as we have set the initial j to 0. The initial-state-selected total reaction cross section values are then obtained by summing over the partial reaction cross section values for the different partial waves:

$$\sigma_{vj}(E) = \frac{\pi}{k^2_{vj}}\sum_{J=0}^{\infty}(2J+1)P^J_{vj}(E) \qquad (15)$$

A damping function[35] was used near the edges in (R, r) space to avoid numerical errors arising from reflection or wrapping around of time-evolved wave packet at the grid edges. It is given by

$$f(X_i) = \sin\left[\frac{\pi}{2}\frac{(X_{mask} + \Delta X_{mask} - X_i)}{\Delta X_{mask}}\right], \quad X_i \geq X_{mask} \qquad (16)$$

activated in the asymptotic R and r channels. X_{mask} ($X = R, r$) is the point at which the damping function is initiated and ΔX_{mask} ($=X_{max} - X_{mask}$) is the width of X over which the function decays from 1 to 0, with X_{max} being the maximum value of X in that direction, in a particular channel. The grid parameters used in the present calculation are listed in Table 1 along with the initial conditions, for $J \leq 8$.

Increase in J adds a substantial centrifugal barrier to the interaction potential resulting in an effective potential that falls off slowly and is no longer negligible at distances considered in Table 1. Therefore, we had to locate the initial WP farther out in the reactant channel for higher J values. We found that for $J > 8$, R_0 had to be increased by 1.0 a_0 on an average for each higher J, keeping in mind a cut off of 0.005 eV for the lowest V_{eff} ($=V(R,r,\gamma) + J(J+1)\hbar^2/2\mu_R R^2$, see eq 1). Consequently, the position of the damping function in the reactant channel also had to be shifted accordingly for each calculation and we needed a longer time evolution of the initial WP to achieve convergence. Converged results were obtained after a total propagation time of 4000−6000 time steps, i.e., 0.97−1.45 ps.

III. Results and Discussion

A. Reaction Probabilities. We have calculated the reaction probability (P^J_{vj}) values summed over different rotational and vibrational levels of the product diatom for the reactants H_2 and D_2 in $v = 0$ and $j = 0$ state over a range of E_{trans} for each integer value of J in the range 0−50 for (H^-, H_2) and (H^-, D_2) collisions and 0−60 for (D^-, H_2) collisions. For all the three systems, for $J = 0$, the reaction probability increases with E_{trans} dramatically near the threshold and then it increases further in steps, before leveling off or declining beyond 1.5 eV as illustrated in Figure 1. For convenience, we have included the internal energy (E_{int}) of H_2 and D_2 and plotted P^J_{00} as a function of total energy ($E = E_{trans} + E_{int}$). For quick reference, the product (H_2 and HD) vibrational (v') energies are indicated as arrows along the x-axis to show how the onset of some of the oscillations in $P^J_{00}(E)$ could arise from the opening up of new product vibrational channels. In addition, there are a number of small oscillations in the $P^J_{00}(E)$ curve, which need to be examined further. The P^J_{00} values for $J = 10$, 20, 30, and 40 included in Figure 1 show how the reaction threshold increases and the oscillations decrease with increase in J. To understand the role of J in determining the reaction cross section, we have plotted the reaction probability (P^J_{00}) and the partial reaction cross section ($(2J+1)P^J_{00}$) values as a function of J at $E_{trans} =$ 1.5 and 3.0 eV in Figure 2. It becomes clear from the figure that our calculated cross section values (see below) are converged for $J = 35$ and 50 for (H^-, H_2) and (H^-, D_2) collisions and $J = 40$ and 60 for (D^-, H_2) collisions for $E_{trans} = 1.5$ and 3.0 eV, respectively.

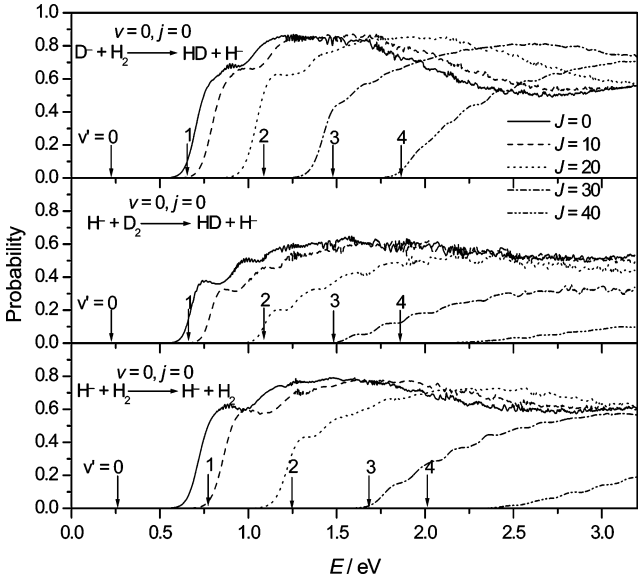

Figure 1. Reaction probability as a function of total energy for different values of J. For convenience the opening up of the different product vibrational channels (v') are indicated by arrows along the x-axis.

B. Reaction Cross Sections. From the results of $P^J_{00}(E)$ values computed for a range of J, we have calculated the integral reaction cross section values for $v = 0$ and $j = 0$, $E_{trans} = 0.3-3.0$ eV, using eq 15. Although the resulting excitation function for (H^-, H_2) collisions plotted in Figure 3 exhibits the same threshold as those of Jaquet and Heinen[23] on the SM PES, our results are significantly lower than theirs for $E \leq 2.5$ eV. This is understandable because Jaquet and Heinen[23] did not carry out the TDQM calculations for $J > 0$. They used the J-shifting approximation, which does not take into account the decline in P^J with increase in J. Interestingly, their results show an unusual increase at higher energies. Unfortunately, there are no experimental results available for (H^-, H_2) collisions.

Our computed results of $\sigma_{00}(E_{trans})$ for H^-, D_2 collisions are compared with the available experimental results in Figure 4.

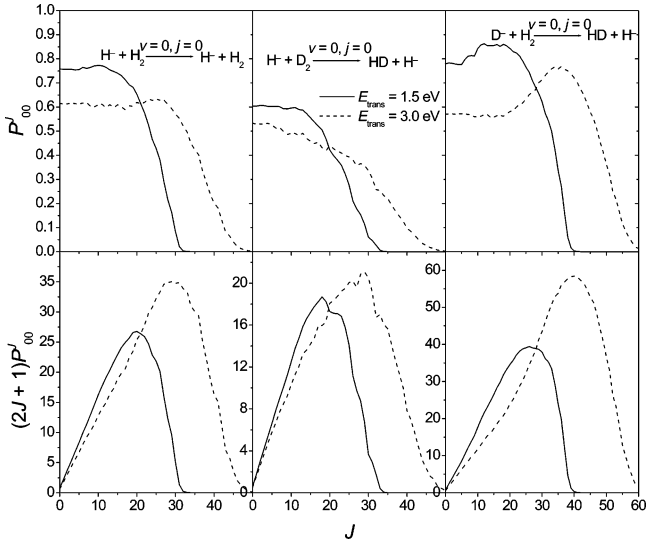

Figure 2. Reaction probability and partial reaction cross section values plotted as a function of J at $E_{trans} = 1.5$ and 3.0 eV.

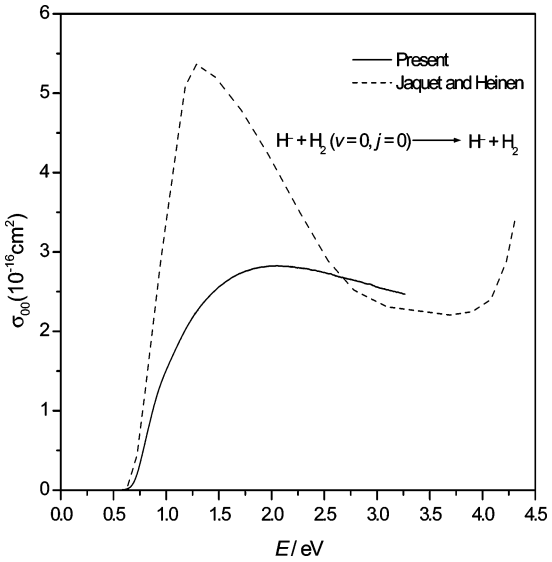

Figure 3. Comparison of the computed integral reaction cross section values on the Panda−Sathyamurthy[24] PES with the calculated values by Jaquet and Heinen[23] on the SM[15] PES for (H^-, H_2 ($v = 0$, $j = 0$)) collisions.

It can be seen that our results are in excellent agreement with the experimental results of Zimmer and Linder[14] for energies below 1.5 eV. Except near the reaction threshold, our results are in general larger than the experimental results by Haufler et al.[16] The reaction cross section results reported by Huq et al.[13] are close to ours at 3.0 eV. Results of Michels and Paulson[12] are significantly lower than ours over the entire energy range. The electron detachment cross section values measured by Huq et al.[13] are also included in Figure 4, indicating the threshold for electron detachment to be around 1.45 eV.

The plot of $\sigma_{00}(E_{trans})$ for D^-, H_2 collisions in Figure 5 show that our results are comparable to the experimental results by Haufler et al.[16] up to ∼0.8 eV, beyond which the theoretical results are always larger than the experimental results. Results of Michels and Paulson[12] are significantly lower than our TDQM results over the entire energy range. The arrow along the *x*-axis indicates the threshold for electron detachment around 1.25 eV for this collision as measured by Huq et al.[13]

To examine the influence of isotopic variation on the reaction cross section we have replotted $\sigma_{00}(E_{trans})$ for (H^-, H_2), (H^-, D_2) and (D^-, H_2) systems in Figure 6, along with the experimental results of Haufler et al.[16] The computed excitation functions show qualitatively the same behavior for all the three systems. That is, a sharp increase at the threshold followed by a maximum around 1.5 eV and then a slight decline. Over the entire energy range, $\sigma_{00}(D^-, H_2) > \sigma_{00}(H^-, H_2) > \sigma_{00}(H^-, D_2)$. Although the experimental results show a sharper decline beyond 1.0 eV, $\sigma_{00}(D^-, H_2)$ is always larger than $\sigma_{00}(H^-, D_2)$. The computed $\sigma_{00}(D^-, H_2)/\sigma_{00}(H^-, D_2)$ hovers around 2.6−3.0 over the entire energy range, while the experimental ratio falls in the range 1.6−2.4 as illustrated in Figure 7.

It is tempting to suggest that the overestimate of $\sigma_{00}(E_{trans})$ by theory over experiment is due to inadequacies in the PES and/or the centrifugal sudden approximation used in the TDQM calculation. The former is unlikely as the Panda−Sathyamurthy PES[26] is of good quality; it includes single, double, and

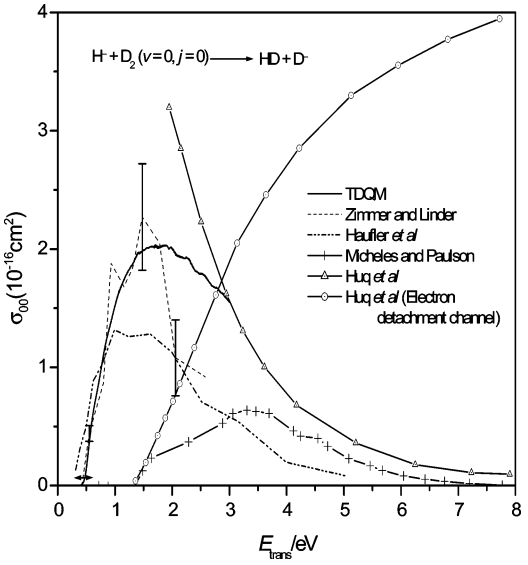

Figure 4. Comparison of the TDQM computed integral reaction cross section values with the different experimental results for (H^-, D_2) collisions. The vertical bars represent the typical error bars in the experimental result of ref 11 and the horizontal double headed arrow indicates the experimental uncertainty in the reaction threshold.

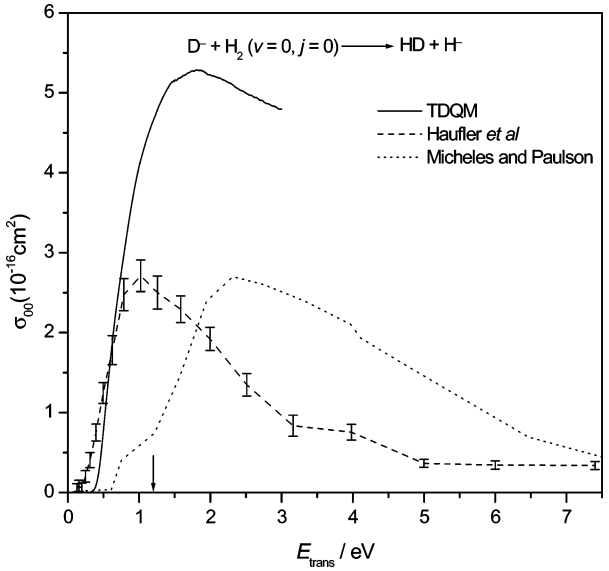

Figure 5. Comparison of the calculated integral reaction cross section values with the experimental results for (D^-, H_2) collisions. Threshold for the electron detachment channel is indicated by an arrow along the *x*-axis.

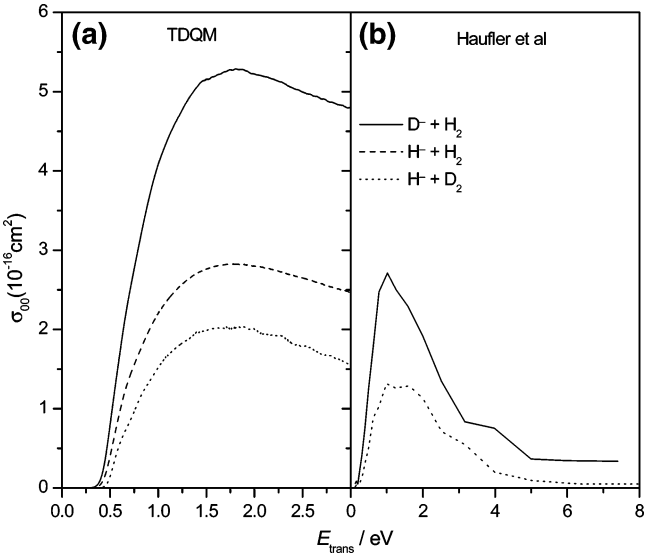

Figure 6. Comparison of the (a) computed and (b) experimental integral reaction cross section for different isotopic combinations.

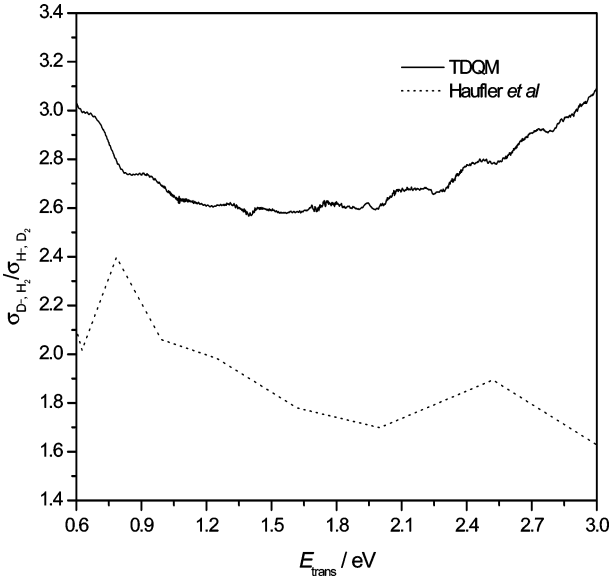

Figure 7. Comparison of the computed ratio of the reaction cross section for (D^-, H_2) to that of (H^-, D_2) collisions with the experimental results by Haufler et al.[13]

nonperturbative triple excitations and is in overall agreement with the SM PES that includes much of the correlation energy. Previous TDQM calculations[25] on the SM PES have been shown to yield results in excellent agreement with the exact time-independent quantum mechanical results for $J = 0$. However, it is possible that for larger J, the neglect of Coriolis coupling could introduce noticeable errors. Our present TDQM results are in excellent accord with the experimental results of Zimmer and Linder for (H^-, D_2) collisions for energies below the threshold for electron detachment channel, even though their experiments involved a rotational temperature (T_{rot}) of 180 K for D_2, while our calculations were restricted to $j = 0$. Therefore, it is likely that, for some reason, the experimental results of Haufler et al. (which used $T_{rot} = 300$ K) tend to underestimate $\sigma_{00}(E_{trans})$ for (H^-, D_2) as well as (D^-, H_2) systems. Interestingly, the thermal rate enhancement for the exchange reactions in (D, H_2) and (H, D_2) collisions was reported to be a factor of 3 by the experimentalists[36] and 2.7 by theorists[37]—somewhat close to the ratio of 2.6−3.0 obtained by us.

IV. Summary and Conclusion

Initial state-selected integral reaction cross section values for 3D collisions in (H^-, H_2) and its isotopic variants have been calculated using the time-dependent quantum mechanical wave packet approach, within the coupled states approximation, on the recently reported ab initio PES. The computed excitation function for $H^- + D_2$ ($v = 0$, $j = 0$) is in excellent agreement with the experimental results of Zimmer and Linder for $E \leq$ 1.5 eV and that of Huq et al. at 3.0 eV. For both (H^-, D_2) and (D^-, H_2) our computed results are significantly larger than the more recent experimental results of Haufler et al. Clearly, more experiments are needed to settle the differences between theory and experiment for this fundamentally important system.

Acknowledgment. The authors are thankful to Dr. D. Gerlich for providing integral reaction cross section values for comparison. K.G. is grateful to the Council of Scientific and Industrial Research (CSIR), New Delhi, for a Fellowship. This study was supported in part by a grant from CSIR, New Delhi.

References and Notes

(1) Carrington, A.; Kennedy, R. A. *J. Chem. Phys.* **1984**, *81*, 91.
(2) Schlier, Ch.; Nowotony, U.; Teloy, E. *Chem. Phys.* **1987**, *111*, 401.
(3) de Polavieia, G. G.; Fulton, N. G.; Tennyson, J. *Mol. Phys.* **1994**, *81*, 92.
(4) Mielke, S. L.; Garrett, B. C.; Peterson, K. A. *J. Chem. Phys.* **2002**, *116*, 4142.
(5) Miller, W. H. *Annu. Rev. Phys. Chem.* **1990**, *41*, 245.
(6) Schatz, G. C. *J. Phys. Chem.* **1996**, *100*, 12839.
(7) Pekeris, C. L. *Phys. Rev.* **1962**, *126*, 1470.
(8) Belyaev, A. K.; Tiukanov, A. S. *Chem. Phys. Lett.* **1999**, *302*, 65.
(9) Stärck, J.; Meyer, W. *Chem. Phys.* **1993**, *176*, 83.
(10) Muschlitz, E. E., Jr.; Bailey, T. L.; Simons, J. H. *J. Chem. Phys.* **1956**, *24*, 1202. Muschlitz, E. E., Jr.; Bailey, T. L.; Simons, J. H. *J. Chem. Phys.* **1957**, *26*, 711.
(11) Mason, E. A.; Vanderslice, J. T. *J. Chem. Phys.* **1958**, *28*, 1070.
(12) Michels, H. H.; Paulson, J. F. In *Potential Energy Surface and Dynamics Calculations*; Truhlar, D. G., Ed.; Plenum: New York, 1981.
(13) Huq, M. S.; Doverspike, L. D.; Champion, R. L. *Phys. Rev. A* **1982**, *27*, 2831.
(14) Zimmer, M.; Linder, F. *Chem. Phys. Lett.* **1992**, *195*, 153. Zimmer, M.; Linder, F. *J. Phys. B* **1995**, *28*, 2671.
(15) Müller, H.; Zimmer, M.; Linder, F. *J. Phys. B* **1996**, *29*, 4165.
(16) Haufler, E.; Schlemmer, S.; Gerlich, D. *J. Phys. Chem. A* **1997**, *101*, 6441.
(17) Belyaev, A. K.; Colbert, D. T.; Groenenboom, G. C.; Miller, W. H. *Chem. Phys. Lett.* **1993**, *209*, 309.
(18) Mahapatra, S.; Sathyamurthy, N.; Kumar, S.; Gianturco, F. A. *Chem. Phys. Lett.* **1995**, *241*, 223.
(19) Balakrishnan, N.; Kalyanaraman, C.; Sathyamurthy, N. *Phys. Rep.* **1997**, *280*, 79.
(20) Zhang, J. Z. H. *Theory and Application of Quantum Molecular Dynamics*; World Scientific: Singapore, 1999.
(21) Mahapatra, S.; Sathyamurthy, N. *J. Phys. Chem.* **1996**, *100*, 2759. Mahapatra, S.; Sathyamurthy, N. *Faraday Discuss. Chem. Soc.* **1998**, *110*, 228.
(22) Ansari, W. H.; Sathyamurthy, N. *Chem. Phys. Lett.* **1998**, *289*, 487.
(23) Gianturco, F. A.; Kumar, S. *J. Chem. Phys.* **1995**, *103*, 2940.
(24) Mahapatra, S. *Phys. Chem. Chem. Phys.* **2000**, *2*, 671.
(25) Jaquet, R.; Heinen, M. *J. Phys. Chem. A* **2001**, *105*, 2738.
(26) Panda, A. N.; Sathyamurthy, N. *J. Chem. Phys.* **2004**, *121*, 9343.
(27) Mowrey, R. C.; Kouri, D. J. *J. Chem. Phys.* **1986**, *84*, 6466.
(28) Mowrey, R. C. *J. Chem. Phys.* **1991**, *94*, 7098. Mowrey, R. C. *J. Chem. Phys.* **1993**, *99*, 7049.
(29) Kosloff, D.; Kosloff, R. *J. Chem. Phys.* **1983**, *52*, 35.
(30) Lill, J. V.; Light, J. C. *Chem. Phys. Lett.* **1982**, *89*, 483. Light, J. C.; Hamilton, I. P.; Lill, J. V. *J. Chem. Phys.* **1985**, *82*, 1400.
(31) Pack, R. T. *J. Chem. Phys.* **1974**, *60*, 633.
(32) Feit, M. D.; Fleck, J. A., Jr.; Steiger, A. *J. Chem. Phys.* **1982**, *47*, 412.
(33) Marston, C. C.; Balint-Kurti, G. G. *J. Chem. Phys.* **1989**, *91*, 3571.
(34) Kalyanaraman, C.; Clary, D. C.; Sathyamurthy, N. *J. Chem. Phys.* **2000**, *113*, 59.
(35) Mahapatra, S.; Sathyamurthy, N. *J. Chem. Soc., Faraday Trans.* **1997**, *93*, 773.
(36) Westenberg, A. A.; de Haas, N. *J. Chem. Phys.* **1967**, *47*, 1393.
(37) Aoiz, F. J.; Bañares, L.; Herrero, V. J.; Sáez Rábanos, V.; Tanerro, I. *J. Phys. Chem. A* **1997**, *101*, 6165.